Biomaterials 35 (2014) 9930–9940

Contents lists available at ScienceDirect

Biomaterials

journal homepage: www.elsevier.com/locate/biomaterials

One-step mixing with humanized anti-mPEG bispecific antibody enhances tumor accumulation and therapeutic efficacy of mPEGylated nanoparticles

Chien-Han Kao [a, 1], Jaw-Yuan Wang [a, b, 1], Kuo-Hsiang Chuang [c], Chih-Hung Chuang [d], Ta-Chun Cheng [c], Yuan-Chin Hsieh [a], Yun-long Tseng [e], Bing-Mae Chen [f], Steve R. Roffler [f, **], Tian-Lu Cheng [d, g, h, *]

[a] Graduate Institute of Medicine, College of Medicine, Kaohsiung Medical University, Kaohsiung 80708, Taiwan
[b] Department of Surgery, Faculty of Medicine, College of Medicine, Kaohsiung Medical University, Kaohsiung 80708, Taiwan
[c] Graduate Institute of Pharmacognosy, Taipei Medical University, Taipei 11031, Taiwan
[d] Department of Biomedical Science and Environmental Biology, Kaohsiung Medical University, Kaohsiung 80708, Taiwan
[e] Taiwan Liposome Company, Ltd., Taipei 11503, Taiwan
[f] Institute of Biomedical Sciences, Academia Sinica, Taipei 11529, Taiwan
[g] Institute of Biomedical Sciences, National Sun Yat-Sen University, Kaohsiung 80424, Taiwan
[h] Center for Biomarkers and Biotech Drugs, Kaohsiung Medical University, Kaohsiung 80708, Taiwan

ARTICLE INFO

Article history:
Received 4 July 2014
Accepted 20 August 2014
Available online 8 September 2014

Keywords:
Bispecific antibody
Methoxy poly(ethylene glycol)
PEGylated nanoparticle
Targeted therapy
Cancer imaging

ABSTRACT

Methoxy PEGylated nanoparticles (mPEG-NPs) are increasingly used for cancer imaging and therapy. Here we describe a general and simple approach to confer tumor tropism to any mPEG-NP. We demonstrate this approach with humanized bispecific antibodies (BsAbs) that can bind to both mPEG molecules on mPEG-NPs and to EGFR or HER2 molecules overexpressed on the surface of cancer cells. Simple mixing of BsAbs with mPEG-NPs can mediate preferential binding of diverse mPEG-NPs to cancer cells that overexpress EGFR or HER2 under physiological conditions and significantly increase cancer cell killing by liposomal doxorubicin to $EGFR^+$ and $HER2^+$ cancer cells. BsAbs modification also enhanced accumulation of fluorescence-labeled NPs and significantly increased the anticancer activity of drug-loaded NPs to antigen-positive human tumors in a mouse model. Anti-mPEG BsAbs offer a simple one-step method to confer tumor specificity to mPEG-NPs for enhanced tumor accumulation and improved therapeutic efficacy.

1. Introduction

Covalent attachment of poly(ethylene glycol) (PEGylation) to nanoparticles (NPs) such as liposomes, micelles, mesoporous silica, carbon nanotubes, quantum dots and SPIOs can increase drug bioavailability, enhance blood circulation half-life [1] and avoid capture by the reticuloendothelial system (RES) [2–4]. These favorable attributes have led to the widespread use of PEGylation in the development of NPs including those already in clinical use such as pegylated liposomal doxorubicin (Caelyx®) for the treatment of Kaposi's sarcoma and ovarian and breast carcinomas [5] and Genexol-PM® (Paclitaxel-loaded mPEG-PLA micelles), approved in South Korea for the treatment of patient's suffering from metastatic breast cancer, non-small cell lung cancer and ovarian cancer [6]. PEGylated nanoparticles (PEG-NPs) are highly regarded as the second generation of drug delivery systems and are rapidly becoming mainstream therapeutic and imaging agents [7,8].

PEG-NPs can accumulate in tumors due to the enhanced permeability and retention (EPR) effect caused by the abnormal structure of endothelial cells in tumors [9,10]. PEG-NPs, however, often accumulate near tumors but do not penetrate into the tumor mass [11,12], and some drugs cannot easily diffuse from PEG-NPs to

* Corresponding author. Department of Biomedical and Environmental Biology, Kaohsiung Medical University, 100 Shih-Chuan 1st Road, Kaohsiung 80708, Taiwan. Tel.: +886 7 3121101 2697; fax: +886 7 3227508.
** Corresponding author. Institute of Biomedical Sciences, Academia Sinica, 128 Academia Road, Section 2, Taipei 11529, Taiwan. Tel.: +886 2 2652 3079; fax: +886 2 2782 9142.
E-mail addresses: sroff@ibms.sinica.edu.tw (S.R. Roffler), tlcheng@kmu.edu.tw, tlcheng5024@gmail.com (T.-L. Cheng).
[1] C.H.K. and J.Y.W. contributed equally to this work.

http://dx.doi.org/10.1016/j.biomaterials.2014.08.032
0142-9612/

cancer cells [13]. Chemical conjugation of specific ligands to PEG-NPs can increase tumor retention and intracellular uptake [14], with concomitant improvement in therapeutic efficacy [15,16] and imaging sensitivity [17,18]. However, chemical linkage of targeting ligands to PEG-NPs has some unsolved problems. Most functional groups (amino, carboxyl, thiol groups) are abundant in targeting ligands, which can cause loss of function, produce heterogeneous coupling orientations and hinder manufacture of a reproducible product after chemical conjugation [19,20]. In addition, chemical conjugation may alter the structure of nano-carriers and encapsulated drugs [21]. These drawbacks can limit the clinical applicability of targeted NPs.

Bifunctional proteins have been developed to non-covalently modify NPs to help overcome limitations of covalently-modified NPs. For example, recombinant ZZ (IgG Fc-binding motif)-His was used as a bispecific adaptor to attach tumor-specific antibodies to nickel-NTA modified NPs [22]. A protein G (IgG-binding β2 domain)-leucine zipper (positive charge) adaptor protein was also employed to decorate antibodies on negatively charged NPs [23]. Although these methods can help maintain antibody binding activity, the NPs need to be modified to accommodate the different bifunctional adaptors. A method that can maintain a homogeneous orientation of ligand, preserve the structure of PEG-NPs and is reproducible and easy to use may help accelerate the translation of targeted NPs to the clinic.

Here, we developed humanized bispecific antibodies (BsAbs) to target mPEG-NPs to cancer cells. The BsAbs were created by fusing the Fab fragment of a humanized anti-mPEG antibody to single-chain antibodies (scFv) with specificity to the EGFR or HER2 tumor antigens. The anti-mPEG portion of the BsAbs was designed to bind to the methoxy ends of mPEG molecules on the surface of mPEG-NPs, leading to homogeneous orientation of the anti-cancer scFv portion of the BsAbs to allow specific targeting of mPEG-NPs to EGFR or HER2-expressing cancer cells. Here we show that tumor targeting capability can be conferred to mPEG-NPs in a one-step method by mixing BsAbs with mPEG-NPs (Fig. 1).

2. Materials and methods

2.1. Materials

Lipo/DOX® was from TTY Biopharm Co., Ltd., Taipei, Taiwan. Lipo/IR780, a liposomal formulation of DSPC, cholesterol and mPEG-DSPE was generously provided by Prof. Yi-Hung Tsai of the Kaohsiung Medical University, Kaohsiung, Taiwan. SN38/PM (micelles loaded with the anticancer drug SN38) and Lipo/Rho (Rhodamine) were kindly supplied by Prof. Yuan-Hung Hsu of the Industrial Technology Research Institute, Hsinchu, Taiwan. FeOdots (NIMT® FeOdot mPEG) were from Genovis, Lund, Sweden. AuNPs were generously provided by Prof. Yun-Ming Wang of the National Chiao Tung University, Hsinchu, Taiwan. $Qdot_{565nm}$ (Qtracker® non-targeted quantum dots) were from Invitrogen Life Technologies Corporation, NY, USA. Erbitux and Herceptin were gifts from Prof. Jaw-Yuan Wang of the Kaohsiung Medical University, Kaohsiung, Taiwan. G418, paraformaldehyde and poly-L-lysine was from Sigma–Aldrich Corp. (St. Louis, MO).

2.2. Cells and animals

BALB 3T3 cells, GP2-293 retrovirus packaging cells (Clontech, Mountain View, CA), SW480 human colon carcinoma cells, SW620 human colon carcinoma cells, SK-BR-3 human breast adenocarcinoma cells and MDA-MB-468 human breast adenocarcinoma cells were grown in Dulbecco's modified Eagle's medium supplemented with 10% (vol/vol) cosmic calf serum (HyClone, Logan, UT), 1% (vol/vol) penicillin/streptomycin (Invitrogen, Carlsbad, CA) at 37 °C in an atmosphere of 5% (vol/vol) CO_2 in air. Six to eight-week-old nude mice were purchased from the National Laboratory Animal Center, Taipei, Taiwan. Animal experiments were performed in accordance with institute guidelines.

2.3. Construction and expression of bispecific antibodies

Hybridomas secreting anti-mPEG or anti-PEG backbone antibodies were generated by immunizing female BALB/c mice with mPEG or PEG-derivatized proteins as described previously [24]. Anti-mPEG hybridomas were screened by ELISA in ninety-six well plates coated with 1 μg $well^{-1}$ CH_3O-PEG_{750}-NH_2 or NH_2-PEG_{3000}-NH_2 (Sigma–Aldrich), whereas anti-PEG backbone hybridomas were screened in plates coated with 1 μg $well^{-1}$ PEG_{5000}-NH_2. Selected hybridomas were cloned three

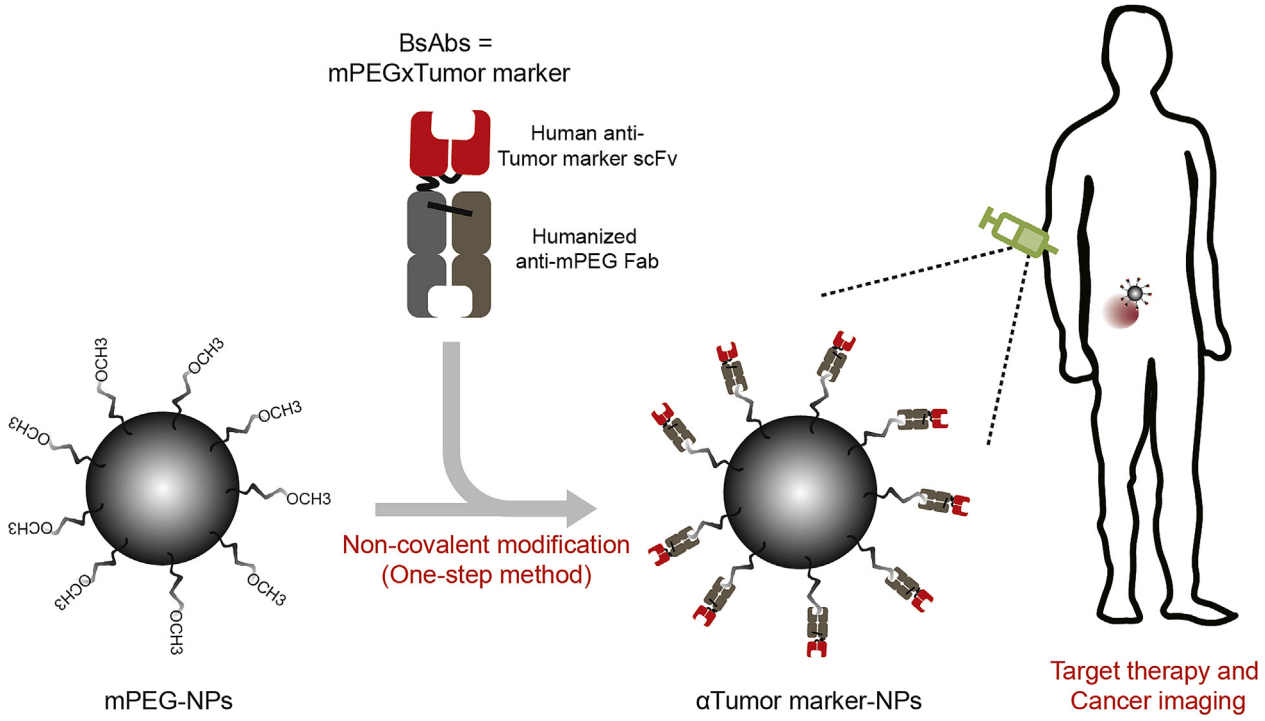

Fig. 1. BsAbs for specific targeting of mPEG-NPs to cancer cells. The humanized 15-2b anti-mPEG Fab fragment was fused to human anti-EGFR or anti-HER2 scFv to form anti-mPEG BsAbs (mPEGxEGFR and mPEGxHER2). The anti-mPEG portion of the BsAb can non-covalently bind to the terminal methoxy portion of mPEG molecules on mPEG-NPs, thereby positioning the anti-EGFR or anti-HER2 scFv outward from the surface of the mPEG-NP. This one-step method can endow non-targeted NP with tumor tropism for specific cancer imaging and therapy.

times by limiting dilution in ninety-six well plates containing thymocyte feeder cells in HT medium (Sigma–Aldrich) supplemented with 15% (vol/vol) fetal calf serum (Hyclone), to obtain 15-2b (anti-mPEG) or 6-3 (anti-PEG backbone) hybridomas. The V_L-$C_κ$ and V_H-C_{H1} domains of the anti-mPEG antibody were cloned from cDNA isolated from the 15-2b hybridoma and were humanized as described previously [25]. The humanized anti-mPEG Fab domain was subcloned into the retroviral vector pLNCX (BD Biosciences, San Diego, CA) in the unique HindIII and SalI restriction enzyme sites. A human anti-EGFR scFv was cloned based on the h528Fv DNA sequence [26] by assembly PCR [27]. Human anti-HER2 scFv and anti-DNS scFv were cloned from the pBub-YCMC plasmid (kindly provided by Prof. Louis M. Weiner of Fox Chase Cancer Center, Philadelphia, PA) [28] and pLNCX-DNS-B7 [29], respectively. A myc tag and fifteen amino acid $(GGGGS)_3$ flexible linker was placed between the anti-mPEG Fab and scFv genes to generate pLNCX-mPEGxEGFR, pLNCX-mPEGxHER2 and pLNCX-mPEGxDNS plasmids. 3T3/mPEGxEGFR, 3T3/mPEGxHER2 or 3T3/mPEGxDNS cells that stably secreted mPEGxEGFR, mPEGxHER2 or mPEGxDNS BsAbs in the culture medium were generated by retroviral transduction as previously described [25]. The producer cells were sorted by FACS on a MoFlo™ XDP (Beckman Coulter, Inc., Brea, CA) at 4 °C to obtain high BsAb productivity [30] and were then cultured in a CELLine (INTEGRA Biosciences AG, Zizers, Switzerland) in 1% (vol/vol) CCS DMEM. The BsAbs were purified by affinity chromatography on gel prepared by reacting 36 mg of o-(2-aminoethyl)-o′-methylpolyethylene glycol 750 (Sigma–Aldrich) per g of CNBr-activated Sepharose™ 4B (GE Healthcare, Little Chalfont, UK). BsAbs (5 μg) were mixed with 6X SDS reducing or non-reducing loading dye (Sigma–Aldrich), boiled for 10 min, electrophoresed on a 10% (wt/vol) SDS-PAGE and stained with Coomassie brilliant blue (Sigma–Aldrich).

2.4. Expression levels of tumor markers on colon and breast cancer cells

EGFR or HER2 expression levels were measured by staining cells with 1 μg ml^{-1} Erbitux or Herceptin, respectively, followed by 1 μg ml^{-1} FITC-conjugated goat anti-human IgG Fc (Jackson ImmunoResearch Laboratories, Westgrove, PA) at 4 °C. After extensive washing with ice-cold PBS containing 0.05% (wt/vol) BSA, the surface immunofluorescence of viable cells was measured with a FACScan flow cytometer (BD Biosciences, San Diego, CA) and fluorescence intensities were analyzed with Cellquest pro software (BD Biosciences).

2.5. BsAb binding to mPEG molecules

Maxisorp 96-well microplates (Nalge-Nunc International, Roskilde, Denmark) were coated with 10 μg ml^{-1} of CH_3O-PEG_{1000}-NH_2 (Creative PEGworks, Winston–Salem, NC), CH_3O-PEG_{750}-NH_2, CH_3O-PEG_{2000}-NH_2, CH_3O-PEG_{5000}-NH_2, CH_3O-PEG_{10000}-NH_2, OH-PEG_{3000}-NH_2 or NH_2-PEG_{3000}-NH_2 (Sigma–Aldrich) in 50 μl well^{-1} 0.1 M $NaHCO_3$ (pH 9.0) for 2 h at 37 °C and then blocked with 200 μl well^{-1} dilution buffer (5% (wt/vol) skim milk in PBS) overnight at 4 °C. 5 μg ml^{-1} of 6-3 anti-PEG backbone Ab or 10 μg ml^{-1} of BsAb (mPEGxEGFR, mPEGxHER2, and mPEGxDNS) in 50 μl 2% (wt/vol) skim milk were added to the plates for 1 h at RT. The plates were washed with PBST (PBS containing 0.05% (vol/vol) Tween-20) three times and with PBS once. 0.5 μg ml^{-1} of mouse anti-HA Ab (Covance, Princeton, NJ) to detect the HA epitiope tag present on the BsAbs was added into the BsAb groups for 1 h at RT. After extensive washing with PBST and PBS, 0.4 μg ml^{-1} of goat anti-mouse IgG Fc-HRP (Jackson ImmunoResearch Laboratories) in 50 μl dilution buffer were added for 1 h at room temperature. The plates were washed with PBS and bound peroxidase activity was measured by adding 150 μl well^{-1} ABTS substrate for 30 min at room temperature. Color development was measured at 405 nm on a microplate reader (Molecular Device, Menlo Park, CA).

2.6. Bi-functional assay of mPEGxEGFR and mPEGxHER2

Ninety-six well plates were coated with 2 μg well^{-1} of poly-L-lysine (40 μg ml^{-1}) in PBS for 5 min at room temperature, washed twice with PBS and then coated with 2×10^5 cells/well of SW480 (EGFR$^+$) or SK-BR-3 (HER2$^+$) cancer cells. mPEGxEGFR, mPEGxHER2 or mPEGxDNS (10 μg ml^{-1}) were added to the wells at room temperature for 1 h. The wells were then washed three times with DMEM and 200 ng ml^{-1} of Lipo/DOX®, 66.7 ng ml^{-1} of Lipo/IR780, 100 ng ml^{-1} of SN38/PM, 600 ng ml^{-1} of FeOdots, 0.5 nM of AuNP or 0.5 nM of $Qdot_{565nm}$ were added to the wells for 20 min. After extensive washing with DMEM, the bound concentrations of PEG-NPs were determined by adding 5 μg ml^{-1} of 6-3 anti-PEG backbone antibody for 1 h, washing with DMEM three times, and then adding 0.4 μg ml^{-1} of goat anti-mouse IgG Fc-HRP (Jackson ImmunoResearch Laboratories). The wells were washed four times with DMEM and then ABTS substrate was added for 30 min before absorbance values at 405 nm were measured in a microplate reader (Molecular Device, Menlo Park, CA).

2.7. Non-covalent modification of mPEG-NPs with BsAbs

BsAbs were added to mPEG-NPs in BSA/PBS buffer (0.05% (wt/vol) BSA in 1× PBS buffer) at 4 °C for 1 h at protein/mPEG-NP ratios of 150 μg BsAb/μmol phospholipid for liposomal drugs, corresponding to approximately 140 BsAbs/liposome based on the assumption that a 100 nm liposome contains ~80,000 phospholipid molecules [31], 550 μg BsAb/μmol FeOdot and 140 ng BsAb/pmol Qdot. mPEG-NPs modified with mPEGxEGFR, mPEGxHER2 or mPEGxDNS are referred to as αEGFR-NPs, αHER2-NPs or αDNS-NPs, respectively.

2.8. BsAbs conversion of non-targeted NPs to targeted NPs

Ninety-six well plates were coated with 2 μg well^{-1} of poly-L-lysine (40 μg ml^{-1}) in PBS for 5 min at room temperature, washed twice with PBS and then each well was coated with 2×10^5 SW480 (EGFR$^+$), SW620 (EGFR$^-$), SK-BR-3 (HER2$^+$) or MDA-MB-468 (HER2$^-$) cancer cells. SW480 (EGFR$^+$) and SW620 (EGFR$^-$) cells were incubated with 4 μg ml^{-1} of αEGFR-Lipo/DOX, 1 μg ml^{-1} of αEGFR-Lipo/IR780 or 4 μg ml^{-1} of αEGFR-FeOdots for 20 min. After extensive washing with DMEM, the presence of bound mPEG-NPs was determined by adding 5 μg ml^{-1} of anti-PEG backbone Ab (6-3) for 1 h, washing the wells with DMEM three times and then adding 0.4 μg ml^{-1} of goat anti-mouse IgG Fc-HRP (Jackson ImmunoResearch Laboratories). The wells were washed four times with DMEM and ABTS substrate was added for 30 min before absorbance values at 405 nm were measured in a microplate reader (Molecular Device, Menlo Park, CA, USA). The same procedure was used to examine binding of αHER2-NPs to SK-BR-3 (HER2$^+$) and MDA-MB-468 (HER2$^-$) cells.

2.9. Characterization of BsAb-Lipo/DOX

The mean particle size, zeta potential and polydispersity index (PDI) of αEGFR-Lipo/DOX, αHER2-Lipo/DOX and Lipo/DOX were analyzed at room temperature using a Zetasizer nano ZS (Malvern, UK). Standard deviations were calculated from at least three measurements. The long-term stability of αEGFR-Lipo/DOX and αHER2-Lipo/DOX was observed by measuring the antigen-binding activity of BsAb-Lipo/DOX after incubation for 0, 24, 48 and 72 h in PBS supplemented with 10% (vol/vol) human serum at 37 °C. Ninety-six well plates were coated with 2 μg well^{-1} of poly-L-lysine (40 μg ml^{-1}) in PBS for 5 min at room temperature, washed twice with PBS and then coated with 2×10^5 SW480 (EGFR$^+$) cells/well or 1×10^5 SK-BR-3 (HER2$^+$) cells/well. Graded concentrations of αEGFR-Lipo/DOX were added to the wells for 20 min. After extensive washing with DMEM, the presence of bound mPEG-NPs was determined by adding 5 μg ml^{-1} of anti-PEG backbone Ab (6-3) for 1 h, washing the wells with DMEM three times and then adding 0.4 μg ml^{-1} of goat anti-mouse IgG Fc-HRP (Jackson ImmunoResearch Laboratories). The wells were washed four times with DMEM and ABTS substrate was added for 30 min before absorbance values at 405 nm were measured in a microplate reader (Molecular Device, Menlo Park, CA, USA). The same procedure was used to examine binding of αHER2-Lipo/DOX to SK-BR-3 (HER2$^+$) cells.

2.10. In vitro cytotoxicity of BsAb-Lipo/DOX

Ninety-six well plates were seeded with 3×10^3 SW480 (EGFR$^+$) or SW620 (EGFR$^-$) cells/well. The next day, the cells were incubated with 2 μg ml^{-1} or 4 μg ml^{-1} of αEGFR-Lipo/DOX, αDNS-Lipo/DOX or Lipo/DOX® at 37 °C for 1 h. The medium was replenished and the cells were incubated 72 h before cell viability was measured with the ATPlite™ Luminescence Assay System (Perkin–Elmer, Inc., Waltham, MA). The same procedure was used for SK-BR-3 (HER2$^+$) and MDA-MB-468 (HER2$^-$) cells incubated with αHER2-Lipo/DOX, αDNS-Lipo/DOX or Lipo/DOX® at 37 °C for 3 h. Results are expressed as percent inhibition of luminescence as compared with untreated cells by the following formula: % inhibition = 100 × (treated luminescence/untreated luminescence). The standard deviation for each data point was averaged over three samples ($n = 3$).

2.11. Confocal microscopy of BsAb-NPs

Circular coverslips (18 mm) in a 12 wells plate were coated with 20 μg well^{-1} of poly-L-lysine (40 μg ml^{-1}) in PBS for 5 min at room temperature. The coverslips were washed twice with PBS and then the coverslips were coated with 4×10^4 SW480 (EGFR$^+$), SW620 (EGFR$^-$), SK-BR-3 (HER2$^+$) or MDA-MB-468 (HER2$^-$) cancer cells. SW480 (EGFR$^+$) and SW620 cells (EGFR$^-$) were incubated with 300 ng ml^{-1} of αEGFR-Lipo/Rho at 37 °C for 1 h. The cells were fixed with 2% (wt/vol) paraformaldehyde in PBS for 30 min at 4 °C and were stained with DAPI for 45 min at 4 °C. The coverslips were washed four times with PBS and then mounted with fluorescent mounting medium (Dako, Glostrup, Denmark) on glass microscope slides. The fluorescent signals of rhodamine were recorded with an Olympus FluoView™ FV1000 confocal microscope (Olympus Imaging America Inc., Center Valley, PA). The same procedure was used to image SK-BR-3 (HER2$^+$) and MDA-MB-468 (HER2$^-$) cells that were stained with 4 nM of αHER2-$Qdot_{565nm}$.

2.12. MR imaging of BsAb-FeOdots

Magnetic resonance (MR) imaging was performed with a clinical 3.0 T MR imager (Signa; GE Healthcare, Little Chalfont, UK). 1×10^7 SW480 (EGFR$^+$) or SW620 (EGFR$^-$) cells were incubated with different concentrations of αEGFR-FeOdots or αDNS-FeOdots (7 μM, 14 μM and 28 μM) at 4 °C for 30 min. The cells were washed with PBS three times and then the accumulation of FeOdots was scanned by a T2-weighted fast spin-echo sequence (TR/TE = 2500 ms/60 ms). The same protocol was used to examine localization of αHER2-FeOdots and αDNS-FeOdots at SK-BR-3 (HER2$^+$) and MDA-MB-468 (HER2$^-$) cells.

2.13. In vivo optical imaging of BsAb-Lipo/IR780 and Lipo/IR780

BALB/c nude mice bearing SW480 ($EGFR^+$) and SW620 ($EGFR^-$) tumor (~100 mm^3) in their hind leg regions were intravenously injected with αEGFR-Lipo/IR780, αDNS-Lipo/IR78, or Lipo/IR780 (100 μg per mouse), respectively. Pentobarbital anesthetized mice were imaged with an IVIS spectrum optical imaging system (excitation, 745 nm; emission, 840 nm; Perkin–Elmer, Inc., Waltham, MA) at 24, 48 and 72 h after injection.

2.14. Treatment of $EGFR^+$ and $EGFR^-$ tumors with BsAb-Lipo/DOX and Lipo/DOX®

BALB/c nude mice ($n = 6$) were inoculated s.c. with 4×10^6 SW480 ($EGFR^+$) cells and 1×10^6 SW620 ($EGFR^-$) cells in their right and left hind leg regions, respectively. After tumor sizes reached ~20 mm^3, saline or Lipo/DOX®, αDNS-Lipo/DOX or αEGFR-Lipo/DOX were i.v. administered at 5 mg DOX kg^{-1} once weekly for 3 weeks, for a total dose of 15 mg DOX kg^{-1}. Tumor measurements were performed once a week using calipers, and tumor sizes were calculated using the equation: (length × width × high)/2. Mice were weighed once a week to examine treatment toxicity.

2.15. Statistical significance

Statistical significance of differences between mean values was estimated with JMP 9.0 software (SAS Institute, Inc., Cary, NC) using the nonparametric Mann–Whitney test. *P*-values in the particle size, zeta potential, cytotoxicity assay, and *in vivo* toxicity <0.05 and *P*-values in the *in vivo* treatment <0.01 were considered to be statistically significant.

3. Results

3.1. Expression and function of humanized anti-mPEG BsAbs

Bi-functional antibodies with the ability to bind to both mPEG and tumor antigens on cancer cells were constructed by linking anti-cancer scFv via a flexible peptide to the C-terminus of the Fab fragment of the anti-mPEG antibody 15-2b (Fig. 2A). Their modular structure allows creation of BsAbs with specificity to different tumor antigens. Here, we created three BsAbs: mPEGxHER2 to target the HER2/neu receptor, which is overexpressed in 20–30% of woman with breast cancer, and is often associated with poor prognosis [32], mPEGxEGFR to bind the EGFR, which is frequently overexpressed on 25–82% of colorectal cancers [33] and a negative control mPEGxDNS that binds the small chemical hapten dansyl [29], which is not present on the surface of cancer cells.

Recombinant BsAbs secreted into the culture medium of stable 3T3 producer cells were affinity purified on immobilized mPEG. SDS-PAGE analysis showed that the BsAbs were composed of a H-scFv fragment (56 kDa) and L fragment (35 kDa) under reducing conditions, and a 91 kDa disulfide-linked BsAb under non-reducing conditions (Fig. 2B). The binding specificity of the anti-mPEG Fab portion of the BsAbs was investigated by direct ELISA in microtiter plates coated with PEG molecules possessing different terminal functional groups (CH_3O-PEG_{2000}-NH_2, OH-PEG_{3000}-NH_2 and NH_2-PEG_{3000}-NH_2). Similar amounts of CH_3O-PEG_{2000}-NH_2, OH-PEG_{3000}-NH_2 and NH_2-PEG_{3000}-NH_2 were coated in the 96-well plates as determined by direct ELISA using an anti-PEG antibody (6-3) which can specifically bind to the PEG backbone (Supplementary Fig. S1A). Anti-mPEG BsAbs selectively bound to CH_3O-PEG_{2000}-NH_2 as compared to OH-PEG_{3000}-NH_2 and NH_2-PEG_{3000}-NH_2 (Supplementary Fig. S1B), indicating that the anti-mPEG BsAbs bind to the methoxy terminus of mPEG. Anti-mPEG BsAbs could bind to different sizes of mPEG molecules (750, 1000, 2000, 5000 and 10,000 Da) (Supplementary Fig. S1C).

Bi-functional binding of the BsAbs was examined by first incubating SW480 colon cancer cells ($EGFR^+$) or SK-BR-3 breast cancer cells ($HER2^+$) cells (Supplementary Fig. S2) with BsAbs, extensively washing unbound BsAbs from the cells, and then detecting if various mPEG-NPs (Lipo/DOX®, Lipo/IR780, SN38/PM, FeOdot, AuNP, and $Qdot_{565nm}$) were retained on the cells. The specific mPEGxEGFR but not the negative control mPEGxDNS BsAb mediated binding of all tested mPEG-NPs to $EGFR^+$ SW480 cancer cells (Fig. 2C). Likewise, mPEGxHER2 but not mPEGxDNS BsAb directed mPEG-NPs to $HER2^+$ SK-BR-3 cancer cells (Fig. 2D). We conclude that both mPEGxEGFR and mPEGxHER2 display bi-functional binding activity to mediate selective delivery of mPEG-NPs to cells that express the EGFR or HER2 tumor markers, respectively.

3.2. Conversion of non-targeted mPEG-NPs to targeted mPEG-NPs

We next examined if simply mixing mPEGxEGFR or mPEGxHER2 with mPEG-NPs could confer cancer cell specificity to the mPEG-NPs. In this study, we included two cell lines that do not express EGFR or HER2 (SW620 colon cancer cells and MDA-MB-468 breast cancer cells, Supplementary Fig. S2) as controls. mPEGxEGFR, mPEGxHER2 or mPEGxDNS were added to various mPEG-NPs (Lipo/DOX®, Lipo/IR780, FeOdots or $Qdot_{565nm}$) to generate targeted αEGFR-NPs, αHER2-NPs or control αDNS-NPs. The αEGFR-NPs bound to SW480 ($EGFR^+$) but not SW620 ($EGFR^-$) tumor cells, demonstrating antigen-specific binding of the targeted NPs (Fig. 3A). mPEG-NPs targeting depended on the anti-EGFR portion of the BsAb since the control αDNS-NPs did not bind to either SW480 ($EGFR^+$) or SW620 ($EGFR^-$) tumor cells. Likewise, incubation of mPEG-NPs with mPEGxHER2, but not control mPEGxDNS BsAb, conferred NP specificity for SK-BR-3 ($HER2^+$) tumor cells, but not MDA-MB-468 ($HER2^-$) tumor cells (Fig. 3B). These results demonstrate that mixing mPEGxEGFR or mPEGxHER2 with mPEG-NPs can endow the NPs with specificity to EGFR or HER2 on cancer cells.

3.3. Characterization of BsAb-Lipo/DOX

To characterize BsAb modified Lipo/DOX®, we examined the base properties of liposomes after incubation with BsAbs. The resultant αEGFR-Lipo/DOX and αHER2-Lipo/DOX were sized at 101.9 ± 1.2 nm and 105 ± 2 nm (mean ± SD; $n = 3$), which were larger than Lipo/DOX® (98.8 ± 0.6; $P > 0.05$). The polydispersity index (P.D.I.) values for all particles were around 0.2 (Supplementary Table S1). These results indicate that attachment of BsAb to Lipo/DOX® increased the particle size without affecting the overall particle size distribution. The zeta potential of αEGFR-Lipo/DOX and αHER2-Lipo/DOX were −48.9 ± 3.0 mA and −50.8 ± 1.8 mA (mean ± SD; $n = 3$), which were more negative than Lipo/DOX® (−43.4 ± 0.6 mA; $P > 0.05$) (Supplementary Table S1). The increase in zeta potential after the incorporation of Ab is consistent with other reports [34].

We also examined the stability of BsAb modified Lipo/DOX® under physiological conditions. αEGFR-Lipo/DOX and αHER2-Lipo/DOX were incubated in 10% human serum at 37 °C for up to 72 h. As control groups, serum-exposed samples were immediately placed on ice to represent the 0 h time point. After incubation, the samples were incubated with antigen-positive cells to determine if antigen-binding activity was maintained. Supplementary Fig. S3A shows that αEGFR-Lipo/DOX retained the ability to bind to SW480 ($EGFR^+$) cells even after 72 h in the presence of serum at 37 °C. Likewise, αHER2-Lipo/DOX retained HER2 specificity to SK-BR-3 ($HER2^+$) cells after incubation in serum for 72 h at 37 °C (Supplementary Fig. S3B). These results indicate that BsAb modified Lipo/DOX® was stable for at least 72 h under physiological conditions.

3.4. Cytotoxicity of αEGFR-Lipo/DOX and αHER2-Lipo/DOX to cancer cells

We investigated whether mPEGxEGFR, mPEGxHER2 or mPEGxDNS could enhance the cytotoxicity of Lipo/DOX® to antigen-positive cancer cells. Indeed, αEGFR-Lipo/DOX produced significantly more cytotoxicity to SW480 ($EGFR^+$) cancer cells as

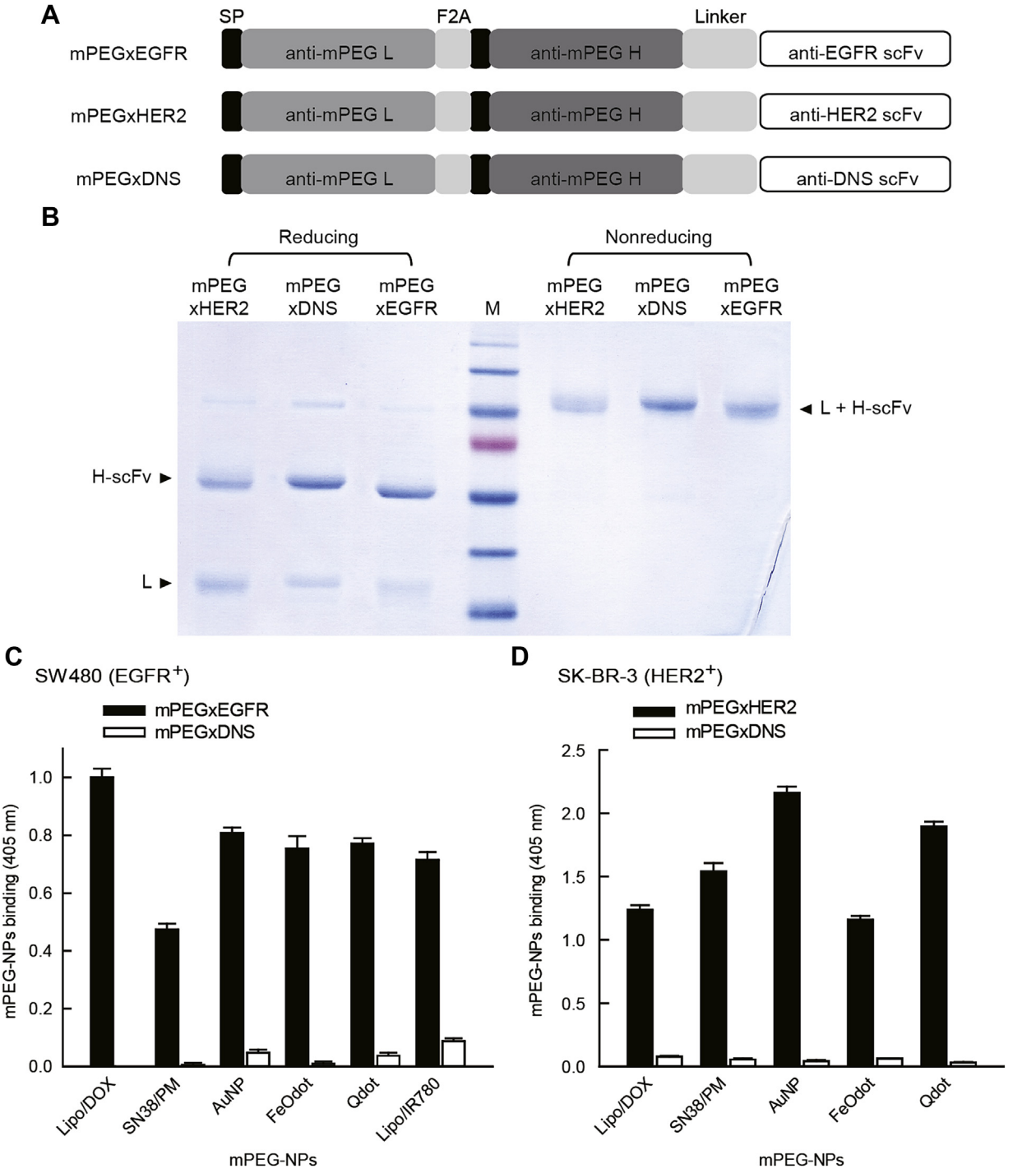

Fig. 2. Characteristics of BsAbs. (A) DNA constructs for humanized BsAbs encode a signal peptide (SP), the anti-mPEG light chain (L), a F2A bicistronic element, the anti-mPEG heavy chain (H), a 15 amino acid flexile linker peptide (Linker) and an anti-EGFR scFv (mPEGxEGFR), anti-HER2 scFv (mPEGxHER2) or control anti-dansyl scFv (mPEGxDNS), respectively. (B) Reducing (left) and non-reducing (right) SDS-PAGE of purified BsAbs. Lane 4 shows a PageRuler™ Prestained Protein Ladder (from bottom to top: 35, 40, 55, 70, 100, 130 and 170 kDa, respectively). (C) SW480 ($EGFR^+$) cancer cells in 96-well plates were incubated with mPEGxEGFR (black bars) or mPEGxDNS (white bars), washed and then incubated with the indicated mPEG-NPs. After washing, bound NPs were detected by ELISA. Results show the mean absorbance values of triplicate determinations. Bars, SD. (D) The ability of mPEGxHER2 (black bars) and mPEGxDNS (white bars) to retain mPEG-NPs at SK-BR-3 ($HER2^+$) cancer cells was determined as in (C).

compared with Lipo/DOX® or αDNS-Lipo/DOX (Fig. 4A). By contrast, αEGFR-Lipo/DOX displayed similar cytotoxicity as Lipo/DOX® and αDNS-Lipo/DOX to SW620 ($EGFR^-$) tumor cells (Fig. 4B), demonstrating that enhanced cytotoxicity induced by αEGFR-NPs requires the presence of the proper tumor antigen (EGFR). Likewise, αHER2-Lipo/DOX was significantly more cytotoxic than Lipo/DOX® and αDNS-Lipo/DOX to SK-BR-3 ($HER2^+$) cancer cells (Fig. 4C) but displayed similar cytotoxicity as Lipo/DOX® and αDNS-Lipo/DOX to MDA-MB-468 ($HER2^-$) cancer cells (Fig. 4D). We conclude that BsAbs can confer tumor selectivity and increase the cytotoxicity of a PEG-NP (Lipo/DOX®) to antigen-positive cancer cells.

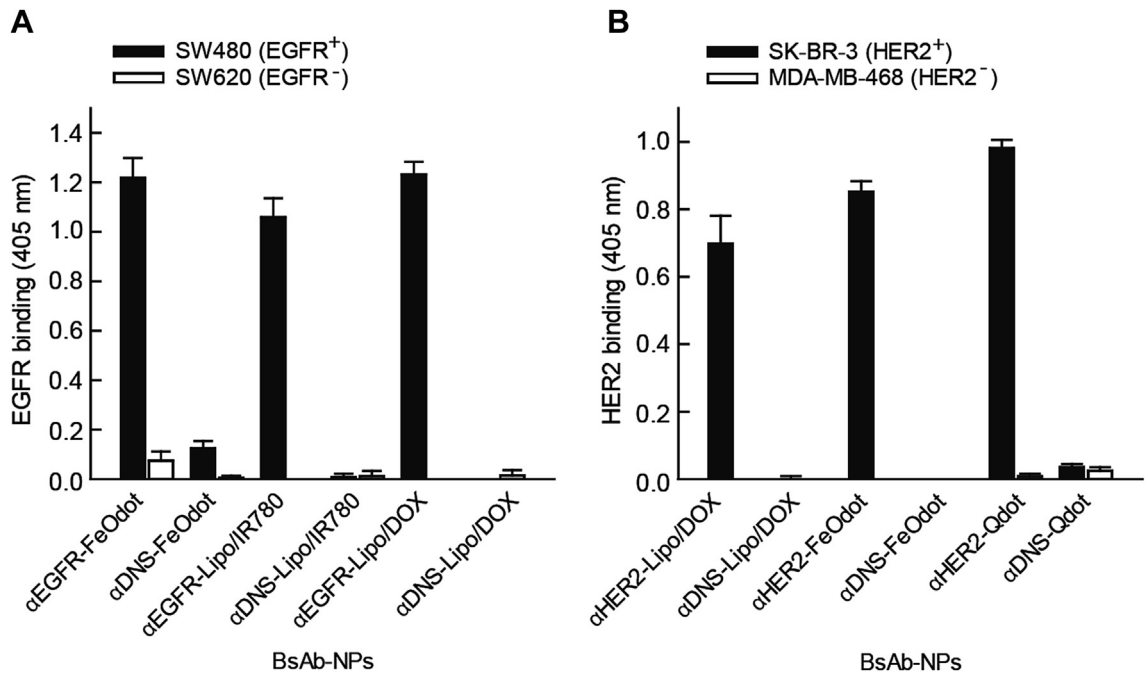

Fig. 3. Cancer cell selectivity of mPEG-NPs modified with BsAbs. (A) FeOdots, Lipo/IR780 and Lipo/DOX® were modified with mPEGxEGFR or control mPEGxDNS BsAb at 4 °C for 1 h at protein/mPEG-NP ratios of 550 μg BsAb/μmol FeOdot, and 150 μg BsAb/μmol phospholipid (for Liposomal drug) before addition to SW480 ($EGFR^+$) or SW620 ($EGFR^-$) cancer cells. mPEG-NP binding to the cells was determined by ELISA ($n = 3$). Bars, SD. (B) Lipo/DOX®, FeOdots and $Qdot_{565nm}$ were treated with mPEGxHER2 or control mPEGxDNS BsAb at protein/mPEG-NP ratios of 150 μg BsAb/μmol phospholipid (for Liposomal drug), 550 μg BsAb/μmol FeOdot, and 140 ng BsAb/pmol Qdot before addition to SK-BR-3 ($HER2^+$) or MDA-MB-468 ($HER2^-$) cancer cells. mPEG-NP binding to the cells was determined by ELISA ($n = 3$). Bars, SD.

3.5. *In vitro imaging of αEGFR-NPs and αHER2-NPs*

Cell imaging was performed by mixing BsAbs with the PEG-imaging probes Lipo/Rho (Rhodamine), $Qdot_{565nm}$ or FeOdots and then examining probe localization in cancer cells by confocal microscopy and magnetic resonance (MR) imaging. Confocal microscopy of αEGFR-Lipo/Rho added to SW480 ($EGFR^+$) and SW620 ($EGFR^-$) cancer cells showed that a red fluorescence signal was only detected on SW480 cells (Fig. 5A). In an analogous fashion, αHER2-$Qdot_{565nm}$ was visualized in SK-BR-3 ($HER2^+$) cells but not MDA-MB-468 ($HER2^-$) tumor cells (Fig. 5B), demonstrating selective binding and uptake of NPs decorated with the appropriate BsAb.

To examine if MR imaging agents could be targeted by BsAbs, different concentrations of αEGFR-FeOdots, αHER2-FeOdots and αDNS-FeOdots were added to SW480 ($EGFR^+$), SW620 ($EGFR^-$), SK-BR-3 ($HER2^+$) and MDA-MB-468 ($HER2^-$) cancer cells. Strong MR signals as visualized by a darker color were only observed for αEGFR-FeOdots and αHER2-FeOdots mixed with SW480 ($EGFR^+$) and SK-BR-3 ($HER2^+$) cancer cells, respectively (Supplementary Fig. S4), demonstrating that BsAbs can confer cancer cell selectivity to MR imaging agents.

3.6. *Specific targeting of αEGFR-Lipo/IR780 in vivo*

To investigate tumor targeting of BsAbs-NPs *in vivo*, BALB/c nude mice bearing $EGFR^-$ SW620 (left side) and $EGFR^+$ SW480 (right side) tumors in their hind leg regions were intravenously injected with αEGFR-Lipo/IR780, αDNS-Lipo/IR780 or Lipo/IR780. Imaging of the mice on an IVIS Spectrum optical imaging system at 24, 48 and 72 h after injection revealed that the fluorescent signal of αEGFR-Lipo/IR780 was enhanced in SW480 ($EGFR^+$) tumors as compared to SW620 ($EGFR^-$) tumors from 24 to 72 h after probe injection (Fig. 6, bottom row). The fluorescent intensity of αEGFR-Lipo/IR780 in SW480 ($EGFR^+$) tumors was 2.04, 2.32 and 2.33-fold greater at 24, 48 and 72 h than in SW620 ($EGFR^-$) tumors, respectively (Supplementary Table S2). By contrast, Lipo/IR780 and αDNS-Lipo/IR780 localized more strongly in SW620 tumors, presumably due to the EPR effect. These data indicate that αEGFR-Lipo/IR780 possessed selectivity for $EGFR^+$ cancer cells, thereby facilitating enhanced accumulation in $EGFR^+$ tumors.

3.7. *mPEGxEGFR can enhance the anticancer activity of Lipo/DOX® to $EGFR^+$ tumors*

To examine whether mPEGxEGFR can increase the therapeutic efficacy of Lipo/DOX® to $EGFR^+$ tumors *in vivo*, we treated BALB/c nude mice bearing SW480 ($EGFR^+$) and SW620 ($EGFR^-$) tumors in their hind leg regions with Lipo/DOX®, αEGFR-Lipo/DOX, αDNS-Lipo/DOX or vehicle alone. αEGFR-Lipo/DOX suppressed the growth of SW480 ($EGFR^+$) tumors significantly more than did Lipo/DOX® ($P < 0.01$ on day 8–43) (Fig. 7A) without any apparent toxicity as assessed by mouse body weight (Fig. 7C). There were no significant differences in the mean sizes of SW620 ($EGFR^-$) tumors in mice treated with αEGFR-Lipo/DOX, αDNS-Lipo/DOX or Lipo/DOX® (Fig. 7B). We conclude that mPEGxEGFR provided tumor tropism and enhanced the anti-tumor efficacy of Lipo/DOX® to $EGFR^+$ tumors *in vivo*. Although mPEGxHER2 appeared to produce greater enhancement of Lipo/DOX® cytotoxicity *in vitro*, we did not test the *in vivo* activity of αHER2-Lipo/DOX because SK-BR-3 tumors, in our hands, failed to reproducibly form xenografts in athymic mice. However, αEGFR-Lipo/DOX displayed significantly greater anti-tumor activity against $EGFR^+$ tumors in mice, demonstrating the utility of this approach.

4. Discussion

Here we describe the development of BsAbs that can confer target-specificity to mPEG-NPs. Anti-mPEG BsAbs are bi-functional

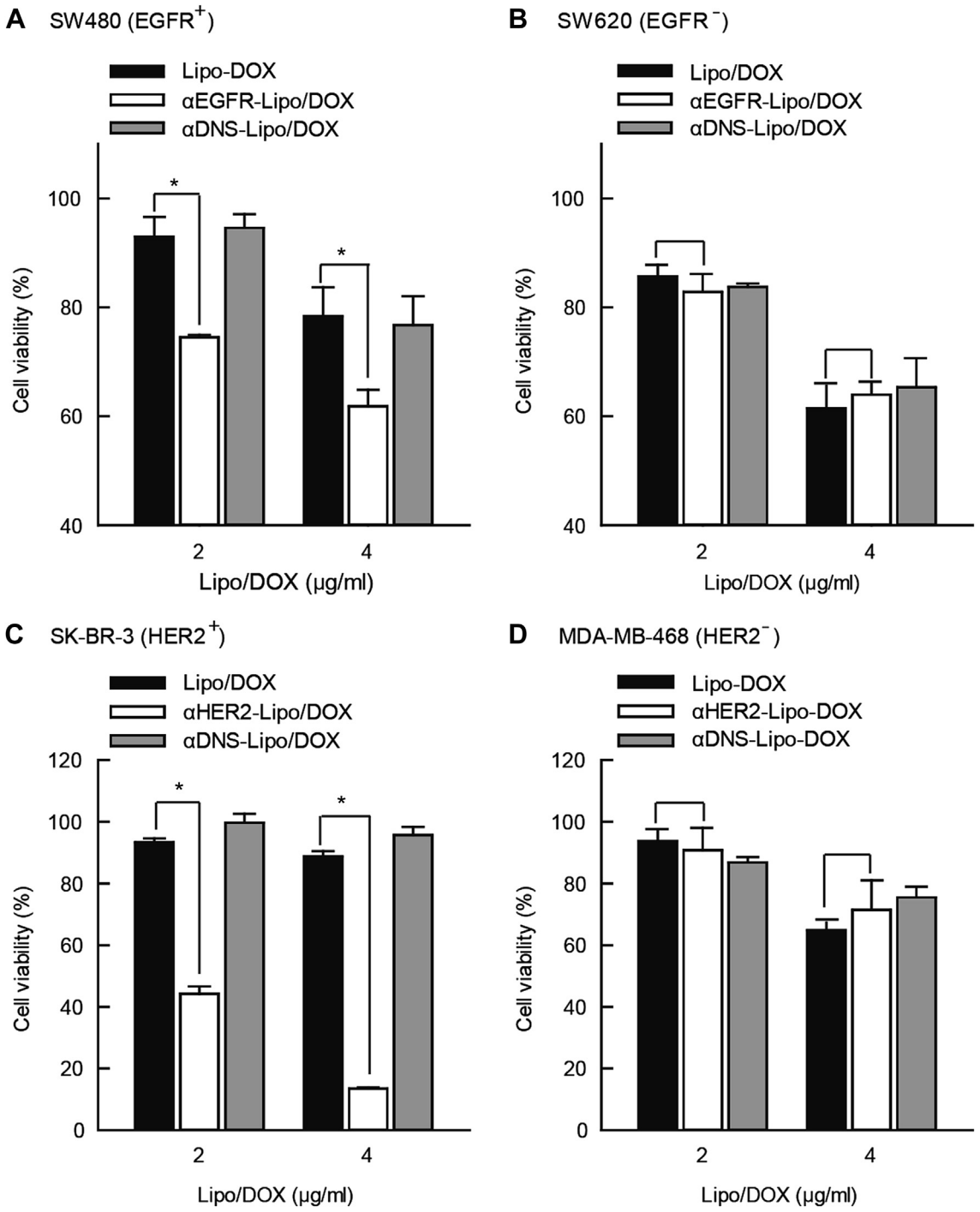

Fig. 4. BsAb modification can enhance the *in vitro* cytotoxicity of Lipo/DOX®. Lipo/DOX® (2 or 4 μg/ml), αEGFR-Lipo/DOX or αDNS-Lipo/DOX were added to (A) SW480 (EGFR$^+$) or (B) SW620 (EGFR$^-$) cancer cells for 1 h. The cells were washed, and then cultured for 72 h before cell viability was determined by ATPlite analysis. In a similar experiment, Lipo/DOX®, αHER2-Lipo/DOX or αDNS-Lipo/DOX were added to (C) SK-BR-3 (HER2$^+$) or (D) MDA-MB-468 (HER2$^-$) cancer cells for 3 h before cell viability was determined 72 h later. Results show mean cell viability compared to untreated control cells ($n = 3$), Bars, SD. *, $P < 0.05$.

modular proteins with the capacity to bind to both mPEG on mPEG-NPs and tumor antigens, such as EGFR or HER2, on cancer cells. The anti-mPEG portion of the BsAb can non-covalently bind to the exposed termini of mPEG molecules to orient the anti-tumor portion of the BsAb outward from the surface of mPEG-NPs, thereby converting non-targeted mPEG-NPs to tumor targeted mPEG-NPs in a one-step method. We show that a wide variety of mPEG-NPs can acquire binding specificity for EGFR or HER2 on cancer cells by simply mixing the BsAbs and mPEG-NPs without the need for disruptive chemical conjugation. The functionality of BsAb modified mPEG-NPs were stable for up to 72 h under physiological conditions. We also demonstrate that mPEGxEGFR can significantly enhance the *in vivo* anticancer activity of Lipo/DOX®, a pegylated liposomal formulation of doxorubicin. This flexible strategy may confer cancer cell selectivity to any PEG-nanodrug or PEG-imaging agent for improved targeted cancer imaging and therapy.

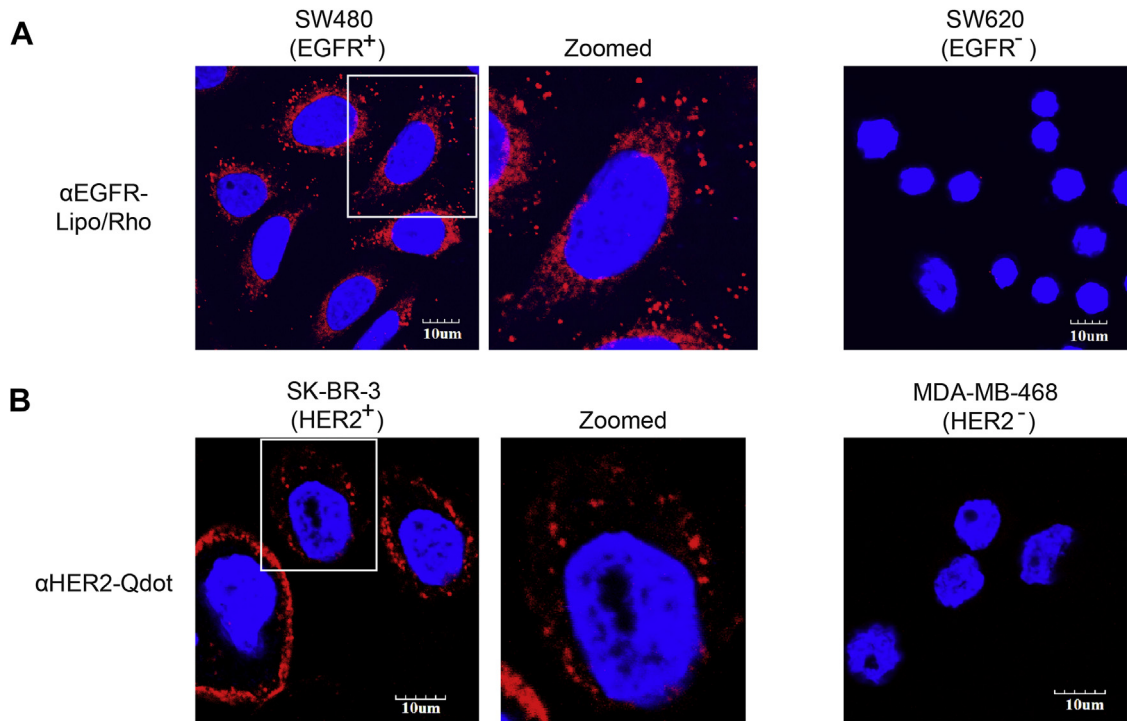

Fig. 5. Cell imaging of BsAb modified NPs. (A) SW480 ($EGFR^+$) and SW620 ($EGFR^-$) cells were incubated with αEGFR-Lipo/Rho (red fluorescence). The cells were fixed, stained with DAPI (blue fluorescence) and then examined under a confocal microscopy. (B) αEGFR-$Qdot_{565nm}$ was added to SK-BR-3 ($HER2^+$) and MDA-MB-468 ($HER2^-$) cells. The cells were processed and visualized as in (A). White scale bars represent 10 μm.

The bispecific antibodies developed in our study were based on our new anti-mPEG antibody 15-2b, which can bind to the terminal methoxy end of mPEG molecules. The BsAbs could also weakly bind to PEG, which possesses a hydroxyl group in place of the larger methoxy group in mPEG, suggesting that the methoxy group participates in antibody binding. BsAbs did not bind to aminoPEG (NH_2-PEG-NH_2) molecules, which may have been caused by binding of both amino groups to the microtiter plates. The binding specificity of 15-2b is clearly different from our previously generated anti-PEG antibodies [24,35,36] and mAb 6.3 (generated in this study), which bind to the repeating ethylene oxide subunits of PEG and therefore bind equally well to PEG, mPEG and aminoPEG. Importantly, the BsAbs could bind to different sizes of mPEG as shown by strong binding to mPEG molecules ranging in size from 750 to 10,000 Da, indicating that they may be useful to target many kinds of mPEG-NPs. Indeed, the BsAbs were able to target a wide range of mPEG-NPs to antigen-positive cancer cells, including liposomes, iron oxide and gold nanoparticles, quantum dots and micelles. Although not studied here, we speculate that the BsAbs may also be useful for targeting mPEGylated proteins and peptides, such as Adagen (PEG-adenosine deaminase), Oncaspar (PEG-asparaginase), Pegasys (peginterferon alpha-2a), PEG-Intron (peginterferon alpha-2b), Somavert (PEG-human growth hormone receptor antagonist), Cimzia (PEG-anti-human TNF-alpha Fab′), Neulasta (PEG-G-CSF), Mircera (PEG-erythropoietin), Macugen (PEG-anti-VEGF aptamer), Pegloticase (PEG-uricase), which are all modified with different sizes of mPEG molecules.

Strategies to confer targeting capability to PEG-NPs have been developed to improve their tumor uptake and therapeutic efficacy. Streptavidin-labeled antibodies can bind biotin-modified PEG molecules on PEG-NPs to enhance uptake into antigen-positive cancer cells [37]. Protein A attached to NPs has also been used to bind intact antibodies to bestow targeting specificity to NPs [38]. However, these methods require multi-step covalent modification of the NPs. More importantly, protein A and streptavidin are immunogenic in humans [39,40], which limits their clinical application. Recently, bispecific antibodies that can bind to the small chemical hapten digoxigenin as well as cell-surface targets have been shown to facilitate cell targeting of small interfering RNA by digoxigenin-PEG modified NPs [41]. By contrast, the BsAbs developed in our study can bind to any mPEG-NP in a one-step method without the need to chemically modify the NP. The BsAbs are constructed from humanized antibody fragments, which display low immunogenicity in patients [42]. Indeed, one-fourth of the antibodies approved for clinical use by the FDA are humanized [43]. Thus, BsAbs can facilitate simple and rapid conversion of non-targeted mPEG-NPs to targeted NPs with low immunogenicity as compared to protein A or streptavidin-based systems.

Site-specific conjugation of antibodies to surfaces produces superior tumor targeting as compared to random conjugation methods that can adversely affect antibody binding to target antigens [44]. Thus, site-specific attachment of antibodies to maintain their proper orientation on PEG-NPs can maximize antigen-binding activity and antitumor activity [19]. Prevalent methods to maintain antibody orientation on NPs include incorporation of maleimide-derivatized PEG molecules on the surface of NPs to allow specific reaction to a cysteine residue engineered into the C-terminus of scFv [45] or integration of a hydrazide group on the PEG terminus to react with previously oxidized carbohydrate chains in the Fc region of intact antibodies [46]. Covalent attachment of scFv or antibodies to PEG-NPs is effective but requires multiple conjugation steps that may alter the physical and pharmacokinetic properties of NPs in undesirable ways [21,47]. The hydrazone linkage also requires a hydrazide-aldehyde reaction which is cytotoxic and can damage biological molecules [20]. By contrast, BsAbs use antibody–antigen

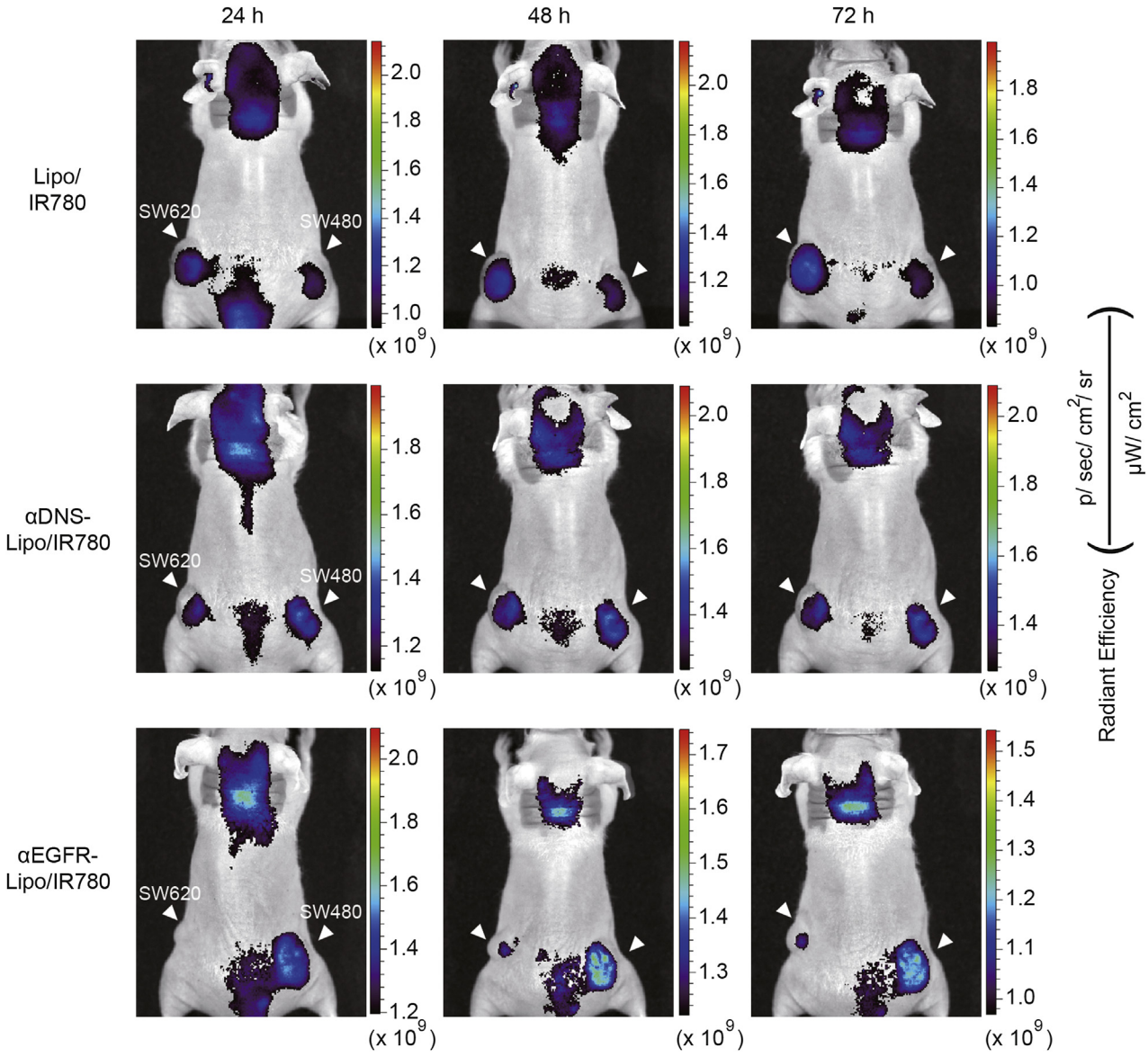

Fig. 6. Imaging of mPEGxEGFR modified Lipo/IR780 *in vivo*. Nude mice bearing EGFR$^-$ SW620 tumors (left flank) or EGFR$^+$ SW480 tumors (right flank) were intravenously injected with 100 μg Lipo/IR780 (top row), 100 μg αDNS-Lipo/IR780 (middle row) or 100 μg αEGFR-Lipo/IR780 (bottom row). Mice were sequentially imaged at 24, 48 and 72 h with an IVIS spectrum optical imaging system.

interactions (non-covalent) [48] to modify mPEG-NPs, minimizing possible alterations of NP properties. We therefore observed minimal changes in the physical properties (particle size, polydispersity and zeta potential) of Lipo/DOX modified with our BsAbs. The BsAbs also bind to the terminal ends of the mPEG chains, thus orienting the anti-tumor scFv portion of the BsAb outward and minimizing steric masking of the BsAbs by PEG [8].

In our study, we developed BsAbs against the EGFR and HER2 and showed that these BsAbs conferred the corresponding tumor specificity to a diverse range of mPEG-NPs. αEGFR-Lipo/DOX displayed significantly greater antitumor activity against EGFR$^+$ tumors in mice, demonstrating the utility of this approach. The mechanism of enhanced anticancer activity is likely due to prolonged retention of the liposomes in tumors (Fig. 6) as well as to receptor-mediated endocytosis of the liposomes into cancer cells (Fig. 5A). We anticipate that BsAbs possessing different tumor marker tropisms, such as against EGFR, HER2, CD20, CD19, CEA, Le^y, mucins and PSMA [43], may facilitate customized therapy depending on the tumor markers displayed on the cancer cells of each patient.

5. Conclusions

In summary, the BsAbs described here possess potential advantages for targeted NP therapy including: 1) Low immunogenicity of humanized Fab and fully human scFv in BsAbs, 2) simple and rapid generation of targeted NPs by mixing BsAbs and NPs, 3) homogenous orientation of BsAbs on NPs via specific binding to the exposed ends of mPEG molecules, 4) minimal impact on NP integrity and stability since chemical conjugation steps are not required to confer targeting specificity, 5) interchangeable specificity of targeting by altering the scFv portion of the BsAbs, allowing customizable adjustment of NP targeting to antigens expressed on each patient's tumor and perhaps extension to development of targeted NPs for other diseases such as cardiac infarction [49] and angiogenesis therapy [50,51], 6) universal applicability to most

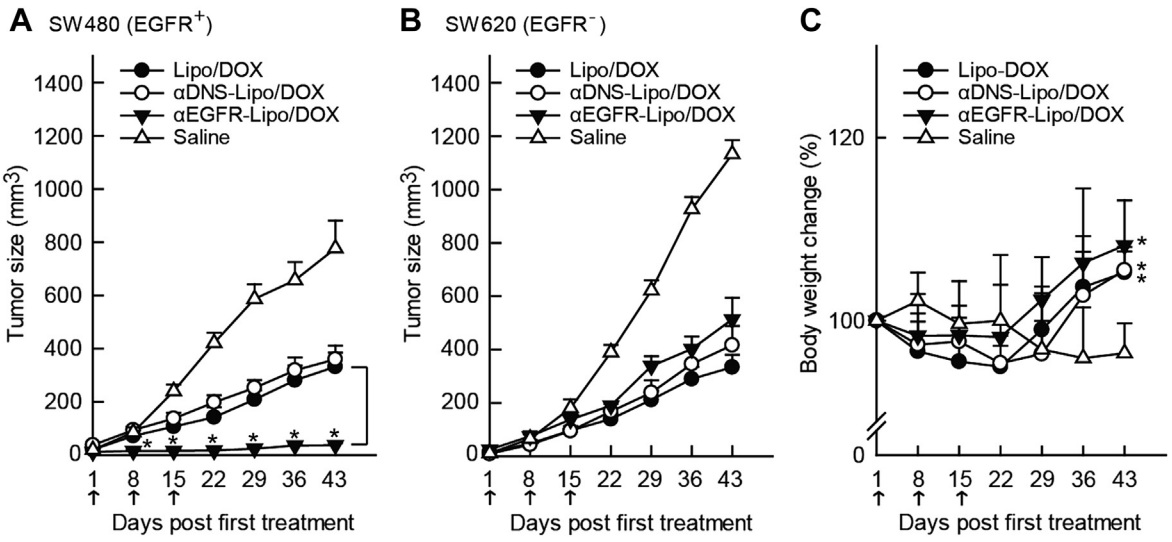

Fig. 7. Therapeutic efficiency of mPEGxEGFR modified Lipo/DOX® against EGFR$^+$ and EGFR$^-$ tumor. Groups of six nude mice bearing EGFR$^+$ SW480 tumors (A) and EGFR$^-$ SW620 tumors (B) were intravenously injected with saline (Δ), 5 mg/kg/dose Lipo/DOX® (●), 5 mg/kg/dose αDNS-Lipo/DOX (○) or 5 mg/kg/dose αEGFR-Lipo/DOX (▼) once a week for 3 weeks (arrows). Results show mean tumor sizes ($n = 6$). Bars, SE. *, $P < 0.01$, comparing αEGFR-Lipo/DOX versus Lipo/DOX® alone. (C) Mean body weights of treated mice during treatment ($n = 6$). $P < 0.05$, comparing αEGFR-Lipo/DOX, αDNS-Lipo/DOX and Lipo/DOX versus saline.

mPEG-NPs and 7) defined stoichiometry since each BsAb binds one mPEG chain, allowing more precise control of antibody loading on NPs. BsAbs therefore offer a simple, rapid, and effective method to confer target specificity to mPEG-NPs.

Acknowledgments

This work was supported by grants from the National Research Program for Biopharmaceuticals, Ministry of Science and Technology, Taipei, Taiwan (MOST 103-2325-B-037-007, NSC102-2321-B-037-001), the Ministry of Health and Welfare, Taiwan (MOHW103-TD-B-111-05), 103NSYSU-KMU Joint Research Project (NSYSUKMU103 I-003), KMU-DT103005, the Grant of Biosignature in Colorectal Cancers, Academia Sinica, Taiwan and the Academia Sinica Research Program on Nanoscience and Nanotechnology.

Appendix A. Supplementary data

Supplementary data related to this article can be found online at http://dx.doi.org/10.1016/j.biomaterials.2014.08.032.

References

[1] Woodle MC, Lasic DD. Sterically stabilized liposomes. Biochim Biophys Acta 1992;1113:171–99.
[2] Alexis F, Pridgen E, Molnar LK, Farokhzad OC. Factors affecting the clearance and biodistribution of polymeric nanoparticles. Mol Pharm 2008;5:505–15.
[3] He Q, Zhang Z, Gao F, Li Y, Shi J. In vivo biodistribution and urinary excretion of mesoporous silica nanoparticles: effects of particle size and PEGylation. Small 2011;7:271–80.
[4] Yang ST, Fernando K, Liu JH, Wang J, Sun HF, Liu Y, et al. Covalently PEGylated carbon nanotubes with stealth character in vivo. Small 2008;4:940–4.
[5] Gabizon AA. Pegylated liposomal doxorubicin: metamorphosis of an old drug into a new form of chemotherapy. Cancer Invest 2001;19:424–36.
[6] Wang AZ, Langer R, Farokhzad OC. Nanoparticle delivery of cancer drugs. Annu Rev Med 2012;63:185–98.
[7] Riggio C, Pagni E, Raffa V, Cuschieri A. Nano-oncology: clinical application for cancer therapy and future perspectives. J Nanomater 2011;2011:17–26.
[8] Jokerst JV, Lobovkina T, Zare RN, Gambhir SS. Nanoparticle PEGylation for imaging and therapy. Nanomedicine 2011;6:715–28.
[9] Maeda H. The enhanced permeability and retention (EPR) effect in tumor vasculature: the key role of tumor-selective macromolecular drug targeting. Adv Enzyme Regul 2001;41:189–207.
[10] Modi S, Jain P, Domb AJ, Kumar N. Exploiting EPR in polymer drug conjugate delivery for tumor targeting. Curr Pharm Des 2006;12:4785–96.
[11] Yuan F, Leunig M, Huang SK, Berk DA, Papahadjopoulos D, Jain RK. Microvascular permeability and interstitial penetration of sterically stabilized (stealth) liposomes in a human tumor xenograft. Cancer Res 1994;54:3352–6.
[12] Jang SH, Wientjes MG, Lu D, Au JLS. Drug delivery and transport to solid tumors. Pharm Res 2003;20:1337–50.
[13] Peer D, Karp JM, Hong S, Farokhzad OC, Margalit R, Langer R. Nanocarriers as an emerging platform for cancer therapy. Nat Nanotechnol 2007;2:751–60.
[14] Bhattacharyya S, Bhattacharya R, Curley S, McNiven MA, Mukherjee P. Nanoconjugation modulates the trafficking and mechanism of antibody induced receptor endocytosis. Proc Natl Acad Sci U S A 2010;107:14541–6.
[15] Kirpotin DB, Drummond DC, Shao Y, Shalaby MR, Hong K, Nielsen UB, et al. Antibody targeting of long-circulating lipidic nanoparticles does not increase tumor localization but does increase internalization in animal models. Cancer Res 2006;66:6732–40.
[16] Pirollo KF, Chang EH. Does a targeting ligand influence nanoparticle tumor localization or uptake? Trends Biotechnol 2008;26:552–8.
[17] Popovtzer R, Agrawal A, Kotov NA, Popovtzer A, Balter J, Carey TE, et al. Targeted gold nanoparticles enable molecular CT imaging of cancer. Nano Lett 2008;8:4593–6.
[18] Satpathy M, Wang L, Zielinski R, Qian W, Lipowska M, Capala J, et al. Active targeting using HER-2-affibody-conjugated nanoparticles enabled sensitive and specific imaging of orthotopic HER-2 positive ovarian tumors. Small 2013;10:544–55.
[19] Manjappa AS, Chaudhari KR, Venkataraju MP, Dantuluri P, Nanda B, Sidda C, et al. Antibody derivatization and conjugation strategies: application in preparation of stealth immunoliposome to target chemotherapeutics to tumor. J Control Release 2011;150:2–22.
[20] Bendas G, Krause A, Bakowsky U, Vogel J, Rothe U. Targetability of novel immunoliposomes prepared by a new antibody conjugation technique. Int J Pharm 1999;181:79–93.
[21] Nobs L, Buchegger F, Gurny R, Allemann E. Current methods for attaching targeting ligands to liposomes and nanoparticles. J Pharm Sci 2004;93:1980–92.
[22] Feng B, Tomizawa K, Michiue H, Miyatake S-i, Han X-J, Fujimura A, et al. Delivery of sodium borocaptate to glioma cells using immunoliposome conjugated with anti-EGFR antibodies by ZZ-His. Biomaterials 2009;30:1746–55.
[23] Goldman ER, Anderson GP, Tran PT, Mattoussi H, Charles PT, Mauro JM. Conjugation of luminescent quantum dots with antibodies using an engineered adaptor protein to provide new reagents for fluoroimmunoassays. Anal Chem 2002;74:841–7.
[24] Su YC, Chen BM, Chuang KH, Cheng TL, Roffler SR. Sensitive quantification of PEGylated compounds by second-generation anti-poly (ethylene glycol) monoclonal antibodies. Bioconjug Chem 2010;21:1264–70.
[25] Chuang K-H, Wang H-E, Cheng T-C, Tzou S-C, Tseng W-L, Hung W-C, et al. Development of a universal anti–polyethylene glycol reporter gene for noninvasive imaging of PEGylated probes. J Nucl Med 2010;51:933–41.
[26] Makabe K, Nakanishi T, Tsumoto K, Tanaka Y, Kondo H, Umetsu M, et al. Thermodynamic consequences of mutations in vernier zone residues of a humanized anti-human epidermal growth factor receptor murine antibody, 528. J Biol Chem 2008;283:1156–66.

[27] Rydzanicz R, Zhao XS, Johnson PE. Assembly PCR oligo maker: a tool for designing oligodeoxynucleotides for constructing long DNA molecules for RNA production. Nucleic Acids Res 2005;33:W521–5.
[28] Shahied LS, Tang Y, Alpaugh RK, Somer R, Greenspon D, Weiner LM. Bispecific minibodies targeting HER2/neu and CD16 exhibit improved tumor lysis when placed in a divalent tumor antigen binding format. J Biol Chem 2004;279:53907–14.
[29] Chuang K-H, Cheng C-M, Roffler SR, Lu Y-L, Lin S-R, Wang J-Y, et al. Combination cancer therapy by hapten-targeted prodrug-activating enzymes and cytokines. Bioconjug Chem 2006;17:707–14.
[30] Brezinsky S, Chiang G, Szilvasi A, Mohan S, Shapiro R, MacLean A, et al. A simple method for enriching populations of transfected CHO cells for cells of higher specific productivity. J Immunol Methods 2003;277:141–55.
[31] Kirpotin D, Park JW, Hong K, Zalipsky S, Li W-L, Carter P, et al. Sterically stabilized anti-HER2 immunoliposomes: design and targeting to human breast cancer cells in vitro. Biochemistry 1997;36:66–75.
[32] Baselga J, Albanell J. Mechanism of action of anti-HER2 monoclonal antibodies. Ann Oncol 2001;12:S35–41.
[33] Spano J, Fagard R, Soria J-C, Rixe O, Khayat D, Milano G. Epidermal growth factor receptor signaling in colorectal cancer: preclinical data and therapeutic perspectives. Ann Oncol 2005;16:189–94.
[34] Gao J, Liu W, Xia Y, Li W, Sun J, Chen H, et al. The promotion of siRNA delivery to breast cancer overexpressing epidermal growth factor receptor through anti-EGFR antibody conjugation by immunoliposomes. Biomaterials 2011;32:3459–70.
[35] Cheng T-L, Cheng C-M, Chen B-M, Tsao D-A, Chuang K-H, Hsiao S-W, et al. Monoclonal antibody-based quantitation of poly (ethylene glycol)-derivatized proteins, liposomes, and nanoparticles. Bioconjug Chem 2005;16:1225–31.
[36] Cheng T-L, Wu P-Y, Wu M-F, Chern J-W, Roffler SR. Accelerated clearance of polyethylene glycol-modified proteins by anti-polyethylene glycol IgM. Bioconjug Chem 1999;10:520–8.
[37] Schnyder A, Krahenbuhl S, Torok M, Drewe J, Huwyler J. Targeting of skeletal muscle in vitro using biotinylated immunoliposomes. Biochem J 2004;377:61.
[38] Jin T, Tiwari DK, Tanaka S-i, Inouye Y, Yoshizawa K, Watanabe TM. Antibody–proteinA conjugated quantum dots for multiplexed imaging of surface receptors in living cells. Mol Biosyst 2010;6:2325–31.
[39] Léonetti M, Thai R, Cotton J, Leroy S, Drevet P, Ducancel F, et al. Increasing immunogenicity of antigens fused to Ig-binding proteins by cell surface targeting. J Immunol 1998;160:3820–7.
[40] Xiao Z, McQuarrie S, Suresh M, Mercer J, Gupta S, Miller G. A three-step strategy for targeting drug carriers to human ovarian carcinoma cells in vitro. J Biotechnol 2002;94:171–84.
[41] Schneider B, Grote M, John M, Haas A, Bramlage B. Targeted siRNA delivery and mRNA knockdown mediated by bispecific digoxigenin-binding antibodies. Mol Ther Nucleic Acids 2012;1:e46.
[42] Hwang WYK, Foote J. Immunogenicity of engineered antibodies. Methods 2005;36:3–10.
[43] Scott AM, Wolchok JD, Old LJ. Antibody therapy of cancer. Nat Rev Cancer 2012;12:278–87.
[44] Rodwell JD, Alvarez VL, Lee C, Lopes AD, Goers J, King HD, et al. Site-specific covalent modification of monoclonal antibodies: in vitro and in vivo evaluations. Proc Natl Acad Sci U S A 1986;83:2632–6.
[45] Lu R-M, Chang Y-L, Chen M-S, Wu H-C. Single chain anti-c-Met antibody conjugated nanoparticles for in vivo tumor-targeted imaging and drug delivery. Biomaterials 2011;32:3265–74.
[46] Koning GA, Kamps JA, Scherphof GL. Efficient intracellular delivery of 5-fluorodeoxyuridine into colon cancer cells by targeted immunoliposomes. Cancer Detect Prev 2002;26:299–307.
[47] Sapra P, Allen T. Ligand-targeted liposomal anticancer drugs. Prog Lipid Res 2003;42:439–62.
[48] Frieden E. Non-covalent interactions: key to biological flexibility and specificity. J Chem Educ 1975;52:754–61.
[49] Dvir T, Bauer M, Schroeder A, Tsui JH, Anderson DG, Langer R, et al. Nanoparticles targeting the infarcted heart. Nano Lett 2011;11:4411–4.
[50] Veeranarayanan S, Poulose AC, Mohamed MS, Varghese SH, Nagaoka Y, Yoshida Y, et al. Synergistic targeting of cancer and associated angiogenesis using triple-targeted dual-drug silica nanoformulations for theragnostics. Small 2012;8:3476–89.
[51] Chen F, Cai W. Tumor vasculature targeting: a generally applicable approach for functionalized nanomaterials. Small 2014;10:1887–93.